Inorganic Chemistry
Article

Inorg. Chem. **2010**, *49*, 11069–11076 **11069**
DOI: 10.1021/ic101619y

First Halogen Anion-Bridged $(MMX)_n$-Type One-Dimensional Coordination Polymer Built upon $d^{10}-d^{10}$ Dimers

Tianle Zhang,*,† Changpeng Ji,† Kaili Wang,† Daniel Fortin,‡ and Pierre D. Harvey*,‡

†*College of Chemistry and Chemical Engineering, Huazhong University of Science and Technology, Wuhan, Hubei 430074, People's Republic of China, and* ‡*Département de Chimie, Université de Sherbrooke, Sherbrooke, Quebec J1K, 2R1, Canada*

Received August 9, 2010

The complex $[Ag_2(PhPPy_2)_2(NCCH_3)_2](ClO_4)_2$ [$PhPPy_2$ = bis(2-pyridyl)phenylphosphine] reacts with NH_4Cl to form an insoluble one-dimensional polymer of the type $(MMX)_n$, $\{[Ag_2(PhPPy_2)_2Cl](ClO_4)\}_n$. The binuclear unit, $Ag_2(PhPPy_2)_2^{2+}$, exhibits two $PhPPy_2$ tridentate ligands bridging the two Ag atoms in a head-to-tail fashion with C_{2h} symmetry, and the Ag···Ag distance [3.0942(11) Å, X-ray] suggests argentophilic interactions. Each Ag center adopts a distorted trigonal-bipyramidal geometry, coordinated by one P atom and two pyridyl arms at the equatorial positions and interacting with one Cl ion and one Ag ion at the axial positions. The short Ag−Cl bond length [2.5791(7) Å] indicates the presence of some covalent character. The solid-state absorption bands spread all the way to 600 nm have been interpreted by means of density functional theory (DFT) and time-dependent DFT (B3LYP), and the lowest-energy excited states are assigned to metal/halide-to-pyridyl charge transfer, consistent with the d^{10} electronic configuration of Ag. The calculated oscillator strengths are low because of the poor molecular orbital overlaps in the charge-transfer components. The novel material exhibits a luminescence band centered at about ∼520 nm.

Introduction

Unidimensional halide-bridged coordination oligomers[1,2] and polymers[3−10] built upon dimetallic fragments, $(MMX)_n$, are of current interest primarily because of their metallic and magnetic properties. From a structural point of view, the construction of these materials is based upon the square-planar geometry about the metal, with the remaining axial positions occupied by the bridging halide and neighboring metal.[11−20] Moreover, species belonging to this same family of halogen-bridged polymers of dimers is a mixed-metal $(Pt_6Rh_2Cl)_n$ polymer in which two dimers are bridged by a Cl ion and two others are not.[21,22] The metal atoms in the $(MMX)_n$ polymers

*To whom correspondence should be addressed. E-mail: tlzhang@mail.hust.edu.cn (T.Z.), Pierre.Harvey@USherbrooke.ca (P.D.H.). Tel: 1-819-821-7092 (P.D.H.). Fax: 86-27-87543632 (T.Z.), 1-819-821-8017 (P.D.H.).

(1) Yin, C.-X.; Huang, G.-C.; Kuo, C.-K.; Fu, M.-D.; Lu, H.-C.; Ke, J.-H.; Shih, K.-N.; Huang, Y.-L.; Lee, G.-H.; Yeh, C.-Y.; Chen, C.-H.; Peng, S.-M. *J. Am. Chem. Soc.* **2008**, *130*, 10090–10092.
(2) Matsunaga, S.; Takizawa, K.; Kawakami, D.; Iguchi, H.; Takaishi, S.; Kajiwara, T.; Miyasaka, H.; Yamashita, M.; Matsuzaki, H.; Okamoto, H. *Eur. J. Inorg. Chem.* **2008**, 3269–3273.
(3) Guijarro, A.; Castillo, O.; Welte, L.; Calzolari, A.; Miguel, P. J. S.; Gómez-Garcia, C. J.; Olea, D.; di Felice, R.; Gómez-Herrero, J.; Zamora, F. *Adv. Funct. Mater.* **2010**, *20*, 1451–1457.
(4) Calzolari, A.; Alexandre, S. S.; Zamora, F.; di Felice, R. *J. Am. Chem. Soc.* **2008**, *130*, 5552–5562.
(5) Iguchi, H.; Takaishi, S.; Miyasaka, H.; Yamashita, M.; Matsuzaki, H.; Okamoto, H.; Tanaka, H.; Kuroda, S. *Angew. Chem., Int. Ed.* **2010**, *49*, 552–555.
(6) Iguchi, H.; Takaishi, S.; Kajiwara, T.; Miyasaka, H.; Yamashita, M.; Matsuzaki, H.; Okamoto, H. *J. Inorg. Organomet. Polym.* **2009**, *19*, 85–90.
(7) Iguchi, H.; Takaishi, S.; Kajiwara, T.; Miyasaka, H.; Yamashita, M.; Matsuzaki, H.; Okamoto, H. *J. Am. Chem. Soc.* **2008**, *130*, 17668–17669.
(8) Yamashita, M.; Takaishi, S.; Kobayashi, A.; Kitagawa, H.; Matsuzaki, H.; Okamoto, H. *Coord. Chem. Rev.* **2006**, *250*, 2335–2346.
(9) Mitsumi, M.; Yoshida, Y.; Kohyama, A.; Kitagawa, Y.; Ozawa, Y.; Kobayashi, M.; Toriumi, K.; Tadokoro, M.; Ikeda, N.; Okumura, M.; Kurmoo, M. *Inorg. Chem.* **2009**, *48*, 6680–6691.
(10) Chaia, Z. D.; Rusjan, M. C.; Castro, M. A.; Donnio, B.; Heinrich, B.; Guillon, D.; Baggio, R. F.; Cukiernik, F. D. *J. Mater. Chem.* **2009**, *19*, 4981–4991.
(11) Kitagawa, H.; Onodera, N.; Ahn, J.-S.; Mitani, T.; Toriumi, K.; Yamashita, M. *Synth. Met.* **1997**, *86*, 1931–1932.
(12) Kitagawa, H.; Onodera, N.; Ahn, J.-S.; Mitani, T.; Kim, M.; Ozawa, Y.; Toriumi, K.; Yasui, K.; Manabe, T.; Yamashita, M. *Mol. Cryst. Liq. Cryst. Sci. Technol., Sect. A* **1996**, 311–316.
(13) Ebihara, M.; Fuma, Y. *Acta Crystallogr., Sect. C: Cryst. Struct. Commun.* **2006**, *62*, m556–558.
(14) Chakravarty, A. R.; Cotton, F. A. *Polyhedron* **1985**, *4*, 1957–1958.
(15) Barral, M. C.; Jiménez-Aparicio, R.; Pérez-Quintanilla, D.; Priego, J. L.; Royer, E. C.; Torres, M. R.; Urbanos, F. A. *Inorg. Chem.* **2000**, *39*, 65–70.
(16) Tejel, C.; Ciriano, M. A.; López, J. A.; Lahoz, F. J.; Oro, L. A. *Organometallics* **1997**, *16*, 4718–4727.
(17) Mitsumi, M.; Kitamura, K.; Morinaga, A.; Ozawa, Y.; Kobayashi, M.; Toriumi, K.; Iso, Y.; Kitagawa, H.; Mitani, T. *Angew. Chem., Int. Ed.* **2002**, *41*, 2767–2771.
(18) Abe, M.; Sasaki, Y.; Yamaguchi, T.; Ito, T. *Bull. Chem. Soc. Jpn.* **1992**, *65*, 1585–1590.
(19) Das, B. K.; Chakravarty, A. R. *Polyhedron* **1991**, *10*, 491–494.
(20) Togano, T.; Mukaida, M.; Nomura, T. *Bull. Chem. Soc. Jpn.* **1980**, *53*, 2085–2086.
(21) Uemura, K.; Yamasaki, K.; Fukui, K.; Matsumoto, K. *Eur. J. Inorg. Chem.* **2007**, 809–815.
(22) Uemura, K.; Fukui, K.; Arai, S.; Matsumoto, K.; Nishikawa, H.; Oshio, H. *Angew. Chem., Int. Ed.* **2005**, *44*, 5459–5464.

Published on Web 11/10/2010

Chart 1

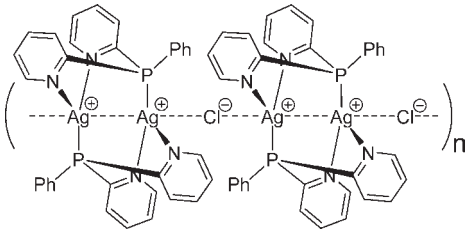

are those capable of forming square-planar or octahedral complexes, and to our knowledge, these are exclusively limited to Ni, Ru, Rh, and Pt.

Recently, one of the authors developed a convenient synthetic route to preparing the tridentate ligand bis(2-pyridyl)-phenylphosphine ($PPhPy_2$)[23] and studied its coordination to transition metals such as Pd, Cu, and Ag.[24−26] In these cases, homo- and heterobimetallic complexes were reported where $PPhPy_2$ acts as a bridging ligand supporting either M−M bonds or M···M interactions. In some cases, luminescence was also detected. We now report a new one-dimensional (1D) coordination polymer of the type $(MMX)_n$, built upon the dimetallic fragment $Ag_2(PPhPy_2)_2^{2+}$ (i.e., $\cdots Ag_2(PPhPy_2)_2^{2+}\cdots Cl^-\cdots Ag_2(PPhPy_2)_2^{2+}\cdots Cl^-\cdots$; Chart 1). This new luminescent material differs from the examples cited above by the fact that the Ag environment is a distorted triangular plane (not a square-planar geometry), where the axial positions are occupied by a Ag atom and a Cl ion. The solid-state photophysical data are supported by density functional theory (DFT) and time-dependent DFT (TDDFT) computations.

Experimental Section

Materials. $[Ag_2(PhPPy_2)_2(CH_3CN)_2](ClO_4)_2$ was prepared according to a literature method.[26] Ammonium chloride, acetonitrile, methanol, and diethyl ether were purchased from commercial sources and used without further purification.

$\{[Ag_2(PhPPy_2)_2Cl](ClO_4)\}_n$. Solid $[Ag_2(PhPPy_2)_2(CH_3CN)_2](ClO_4)_2$ (0.0046 g, 0.0045 mmol) was dissolved in 0.4 mL of acetonitrile, to which a 1 mL methanolic solution of ammonium chloride (0.0095 mol·L^{-1}, 0.0095 mmol) was added with stirring. After 0.5 h, the cloudy solution was filtered to remove the precipitate. The polymer was obtained in about 51% yield as colorless crystals in about 3 weeks by diffusion of diethyl ether onto the filtrate (0.0020 g). Elem anal. Calcd for $C_{32}H_{26}N_4O_4P_2Cl_2Ag_2$: C, 43.72; H, 2.96; N, 6.37. Found: C, 43.28; H, 2.87; N, 6.15. IR: 1088 cm^{-1} [vs, $\nu(ClO_4^-)$].

Physical Measurements. Fourier transform IR spectra were recorded on a Bruker Vertex 70 spectrometer. UV and emission spectra were measured on Perkin-Elmer Lambda 35 and Jasco FP-6500 spectrometers, respectively. Elemental analysis (C, H, N) was determined on a Perkin-Elmer elemental analyzer.

X-ray Structure Determinations. A suitable single crystal with dimensions of 0.30 × 0.20 × 0.15 mm was selected and mounted on the end of a thin glass fiber. Diffraction data were collected on a Bruker SMART APEX CCD-based diffractometer with graphite-monochromated Mo Kα radiation (λ = 0.710 73 Å) at 293 K. The structure was solved by direct methods and refined by full-matrix least squares using the *SHELXTL* crystallographic software package.[27] Anisotropic displacement parameters were applied to all non-H atoms. The H atoms were included and were generated geometrically. A summary of crystallographic data and refinement parameters is given in Table 1.

Table 1. Crystal Data and Collection Parameters for Polymer $\{[Ag_2(PhPPy_2)_2Cl](ClO_4)\}_n$

empirical formula	$C_{32}H_{26}N_4O_4P_2Cl_2Ag_2$
fw	879.15
temp/K	293(2)
cryst syst	monoclinic
space group	*C*2/*m*
a/Å	18.263(4)
b/Å	13.911(3)
c/Å	8.236(2)
α/deg	90
β/deg	100.237(4)
γ/deg	90
volume/$Å^3$	2059.1(9)
Z	2
density(calcd)/g·cm^{-3}	1.444
F(000)	888
μ/mm^{-1}	1.197
reflns collected	7423
unique reflns [*R*(int)]	2108 [*R*(int) = 0.0254]
data/restraints/param	2108/10/132
final R1 [$F > 4\sigma(F)$]	0.0491
wR2 (all data)	0.1610
GOF	1.258

Computations. The electronic structure was calculated using *Gaussian09* software,[28] at Université de Sherbrooke's Mammouth supercomputer, supported by Réseau Québécois de Calcul de Haute Performance. DFT and TDDFT[29−35] were calculated using the B3LYP[33−35] method with 3-21G* basis sets on C, H, N, Cl, and P atoms[36−41] and SBKJC effective-core potentials with VDZ valence double-ζ electrons for Ag.[42−45] All of the geometries were taken directly from the single-crystal structure coordinates; a single-point calculation was performed on each asymmetric unit number in the polymerization direction. The UV−vis spectrum was also computed using *Gaussian* software[46]

(23) Zhang, T.-L.; Qin, Y.; Wu, D.-Y.; Zhou, R.; Yi, X.-W.; Liu, C.-L. *Synth. Commun.* **2005**, *35*, 1889–1895.
(24) Zhang, T.-L.; Qin, Y.; Wu, D.-Y.; Wang, C.-G.; Liu, C.-L. *J. Coord. Chem.* **2005**, *58*, 1485–1491.
(25) Zhang, T.-L.; Chen, C.-G.; Qin, Y.; Meng, X.-G. *Inorg. Chem. Commun.* **2006**, *9*, 72–74.
(26) Zhang, T.-L.; Ji, C.-P.; Wang, K.-L.; Hu, D.-S.; Meng, X.-G.; Chen, C.-G. *Inorg. Chim. Acta* **2007**, *360*, 1609–1615.
(27) (a) Sheldrick, G. M. *SADABS*; University of Göttingen: Göttingen, Germany, 1997. (b) Sheldrick, G. M. SHELXS97 and SHELXL97; University of Göttingen: Göttingen, Germany, 1997.
(28) *Gaussian09*; Gaussian, Inc.: Wallingford, CT, 2009.
(29) Hohenberg, P.; Kohn, W. *Phys. Rev.* **1964**, *136*, B864–B871.
(30) Kohn, W.; Sham, L. J. *Phys. Rev.* **1965**, *140*, A1133–A1138.
(31) *The Challenge of d and f Electrons*; Salahub, D. R., Zerner, M. C., Eds.; American Chemical Society: Washington, DC, 1989.
(32) Parr, R. G.; Yang, W. *Density Functional Theory of Atoms and Molecules*; Oxford University Press: Oxford, U.K., 1989.
(33) Becke, A. D. *J. Chem. Phys.* **1993**, *98*, 5648–5652.
(34) Lee, C.; Yang, W.; Parr, R. G. *Phys. Rev. B: Condens. Matter Mater. Phys.* **1988**, 785–789.
(35) Miehlich, B.; Savin, A.; Stoll, H.; Preuss, H. *Chem. Phys. Lett.* **1989**, *157*, 200–206.
(36) Binkley, J. S.; Pople, J. A.; Hehre, W. J. *J. Am. Chem. Soc.* **1980**, *102*, 939–947.
(37) Gordon, M. S.; Binkley, J. S.; Pople, J. A.; Pietro, W. J.; Hehre, W. J. *J. Am. Chem. Soc.* **1982**, *104*, 2797–2803.
(38) Pietro, W. J.; Francl, M. M.; Hehre, W. J.; Defrees, D. J.; Pople, J. A.; Binkley, J. S. *J. Am. Chem. Soc.* **1982**, *104*, 5039–5048.
(39) Dobbs, K. D.; Hehre, W. J. *J. Comput. Chem.* **1986**, *7*, 359–378.
(40) Dobbs, K. D.; Hehre, W. J. *J. Comput. Chem.* **1987**, *8*, 861–879.
(41) Dobbs, K. D.; Hehre, W. J. *J. Comput. Chem.* **1987**, *8*, 880–893.
(42) *Basis Set Exchange Library* https://bse.pnl.gov/bse/portal.
(43) Stevens, W. J.; Basch, H.; Krauss, M. *J. Chem. Phys.* **1984**, *81*, 6026–6033.
(44) Stevens, W. J.; Krauss, M.; Basch, H.; Jasien, P. G. *Can. J. Chem.* **1992**, *70*, 612–630.
(45) Cundari, T. R.; Stevens, W. J. *J. Chem. Phys.* **1993**, *98*, 5555–5565.
(46) O'Boyle, N. M.; Tenderholt, A. L.; Langner, K. M. *J. Comput. Chem.* **2008**, *29*, 839–845.

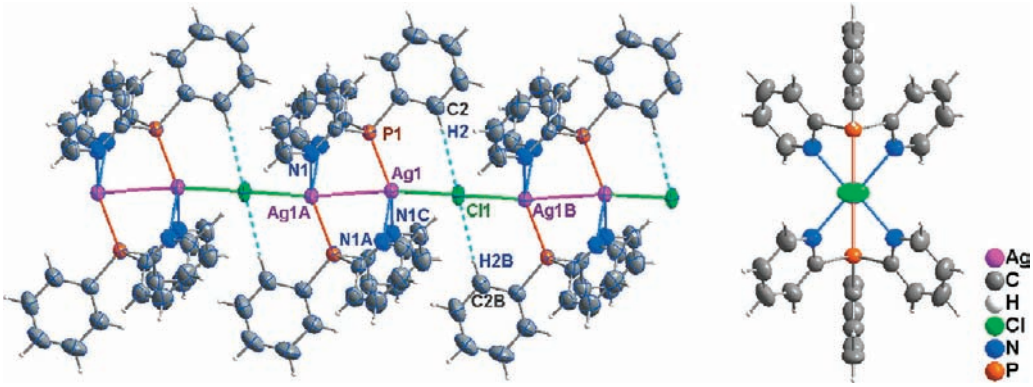

Figure 1. (a) Linear chain structure in the $\{[Ag_2(PhPPy_2)_2Cl](ClO_4)\}_n$ polymer (50% thermal ellipsoids). (b) Linear chain viewed along the *c* direction (50% thermal ellipsoids). Perchlorate groups are omitted for clarity. Symmetry codes: A, $2-x, y, 1-z$; B, $2-x, y, 2-z$; C, $2-x, 2-y, 1-z$. Selected bond distances (Å) and angles (deg): Ag1−Ag1A 3.0942(11), Ag1−Cl1 2.5791(7), Ag1−N1A 2.378(4), Ag1−N1C 2.378(4), Ag1−P1 2.3834(16), H2···Cl1 2.5957(6); Ag1A−Ag1−Cl1 172.48(2), Ag1−Cl1−Ag1B 180.000, P1−Ag1−N1A 133.38(10), P1−Ag1−N1C 133.38(10), N1A−Ag1−N1C 80.65(18), P1−Ag1−Ag1A 73.47(4), P1−Ag1−Cl1 114.04(4), N1A−Ag1−Ag1A 83.01(10), N1C−Ag1−Ag1A 83.01(10), N1A−Ag1−Cl1 91.28(10), N1C−Ag1−Cl1 91.28(10), C2−H2−Cl1 176.645(13), H2−Cl1−H2B 180.000.

with a full-width at half-maximum (fwhm) of 1000 cm^{-1}. The number of $Cl[Ag_2(PhPPy_2)_2Cl]_n$ units was limited to 7 in the DFT computations and 3 in the TDDFT calculations. Attempts to compute larger oligomers failed on our supercomputer.

Results and Discussion

Synthesis. The reaction of the dicationic binuclear complex $[Cu_2(PhPPy_2)_2(NCCH_3)_2](ClO_4)_2$ with 2 equiv of ammonium chloride produces the neutral dinuclear complex $[Cu_2(PhPPy_2)_2Cl_2]$.[47] However, when one uses the silver analogue $[Ag_2(PhPPy_2)_2(NCCH_3)_2](ClO_4)_2$ as the starting material, a similar reaction takes place but, unexpectedly, leads to a new polymer with the formula $\{[Ag_2(PhPPy_2)_2Cl](ClO_4)\}_n$ as determined by X-ray crystallography (see below). This material crystallizes as the sole product, instead of the anticipated binuclear complex $[Ag_2(PhPPy_2)_2Cl_2]$. Upon reduction of the relative amount of ammonium chloride, the colorless title polymer and starting material are always found to cocrystallize as colorless blocks and needles, respectively. The solid-state IR spectrum does not exhibit the characteristic absorption band for coordinated acetonitrile molecules at 2017 cm^{-1} in the starting material, indicating that these coordinated CH_3CN molecules are completely substituted by Cl anions. The strong peak at 1088 cm^{-1} is consistent with the presence of perchlorate counterions in this new material.

The difference in reactivity between the copper and silver binuclear complexes is at first glance difficult to explain. The new polymer, $\{[Ag_2(PhPPy_2)_2Cl](ClO_4)\}_n$, precipitates out of solution during the reaction and is insoluble in most common solvents. We propose that the poor solubility of the mixed-anion-containing polymer causes precipitation to occur before anion exchange is completed. Consequently, the Ag···Cl interactions appear strong (see the comment on the short Ag−Cl distance).

Structural Analysis. Crystallographic studies revealed that the dinuclear complex unit in the polymer is retained, where two bis(2-pyridyl)phenylphosphine ligands bind

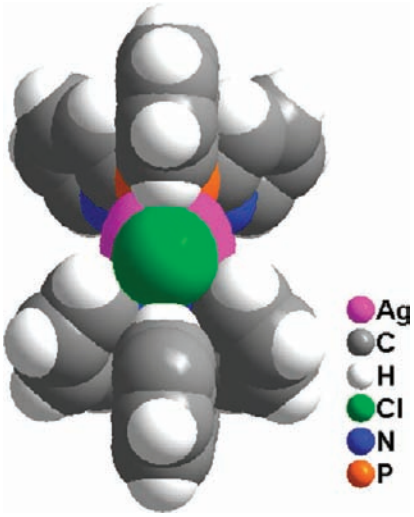

Figure 2. Space-filling plot showing the C−H···Cl interactions in $\{[Ag_2(PhPPy_2)_2Cl](ClO_4)\}_n$.

the two Ag centers in a head-to-tail fashion (Figure1a). Each Ag center adopts a distorted trigonal-bipyramidal geometry, coordinated by one P atom and two pyridyl groups in the equatorial positions and by a Cl ion and a Ag ion in the axial positions. The Ag···Ag distance is 3.0942(11) Å, indicative of the existence of argentophilic interactions.[48] The Ag−Cl bond length [2.5791(7) Å] proves to be short when compared to that cited in the literature,[49] hence suggesting the presence of covalent interactions. These stronger interactions in comparison with a purely ionic bonding may explain the insolubility of the polymer.

The most interesting structural feature of this compound is that these dinuclear units are connected by Cl anions as bridging ligands to generate a 1D chain of the type $(MMX)_n$ (Figure 1a,b). This structural 1D polymer

(47) Zhang, T.-L.; Wang, K.-L; Ng, S.-W. *Acta Crystallogr.* **2005**, *E62*, m3494–3495.

(48) (a) Pyykkö, P. *Chem. Rev.* **1997**, *97*, 597–636. (b) Che, C.-M.; Tse, M.-C.; Chan, M. C. W.; Cheung, K.-K.; Phillip, D. L.; Leung, K.-H. *J. Am. Chem. Soc.* **2000**, *122*, 2464–2468.

(49) (a) Deivaraj, T. C.; Vittal, J. J. *Inorg. Chim. Acta* **2002**, *336*, 111–114. (b) Zhang, H.; Jiang, J.; Yang, N.; Dang, H; Teo, B. T. *J. Cluster Sci.* **1998**, *9*, 547–554. (c) Liu, X.; Guo, G.-C.; Chen, W.-T.; Zhang, Z.-J.; Huang, J.-S. *Dalton Trans.* **2006**, 884–886.

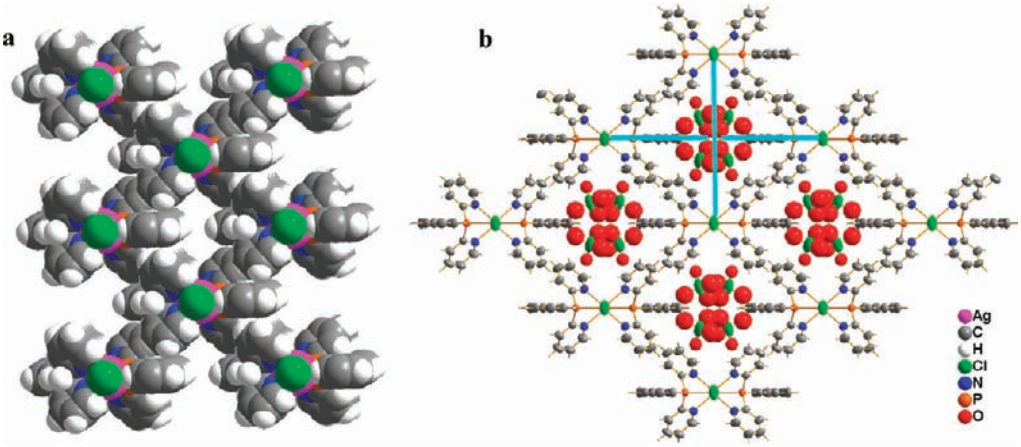

Figure 3. (a) Crystal packing diagram showing the 1D channel along the *c* direction. (b) Packing diagram showing the disorder of the perchlorate groups in the channels. Four possible locations for the perchlorate group in the channel are divided by a turquoise cross.

feature is usually found for nickel, ruthenium, rhodium, and platinum complexes but has never been observed for copper(I) and silver(I) compounds to the best of our knowledge. The closest and only other example is a gold(I) tetramer reported about 2 decades ago, in which two dimeric units were found to be bridged by a Br or an I anion.[50] In the title polymer, the Cl anion is centered between two Ag ions (Ag1−Cl1−Ag1B = 180.00°). However, the angle of Ag1A−Ag1−Cl1 [172.48(2)°] indicates that the polymer chain just slightly deviates from perfect linearity. Finally, the trigonal-bipyramidal geometry about the metal atoms in this type of coordination is also unique because all other reported literature examples exhibit an octahedral geometry for the metal in the $(MMX)_n$ polymers.

Recently, it was demonstrated that weak hydrogen bonds are important in crystal engineering and supramolecular chemistry.[51] In this polymer, the Cl anion interacts with two *o*-H atoms H2 and H2B of the two phenyl groups belonging to neighboring dinuclear silver complex units (Figure 1a). The H···Cl distance is 2.5957(6) Å, which is much shorter than the sum of the van der Waals radii (2.95 Å).[52] Figure 2 clearly shows that two phenyl groups and one Cl anion are arranged in a quasi-perfect straight line [C2−H2−Cl1 = 176.645(13)°], and the close contact between the H and Cl anions appears to play an important role in the construction of this unusual $\{[Ag_2(PhPPy_2)_2Cl](ClO_4)\}_n$ polymer.

In the solid state, the 1D polymer chains are placed parallel to each other, and no interaction between these chains is observed. Four polymer chains aggregate to form a 1D channel (Figure 3a). Crystallographic studies reveal that these channels are filled by the perchlorate anions. The four positions allowing an anion to be placed in these channels are present. These disordered perchlorate anions in these channels are depicted in Figure 3b.

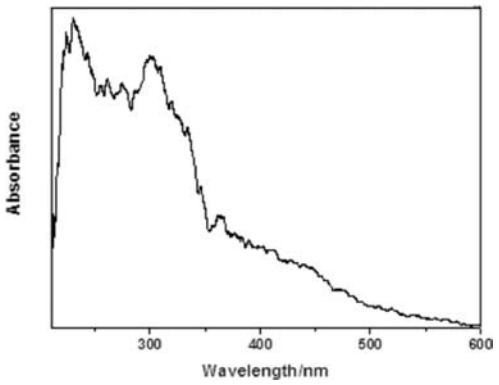

Figure 4. UV spectrum of $\{[Ag_2(PPhPy_2)_2]Cl(ClO_4)\}_n$ in the solid state at 298 K.

Photophysical Study. The polymer exhibits luminescence in the 500 nm region (below). This observation prompted us to analyze the electronic spectrum. Figure 4 shows the solid-state absorption spectrum of this new $\{[Ag_2(PhPPy_2)_2Cl](ClO_4)\}_n$ polymer at 298 K. The absorption spectrum is characterized by a series of stronger features in the 250−350 nm region and a long tail expanding from 350 to 600 nm.

The colorless nature of the insoluble polymer is surprising considering the presence of absorption features in the 400 nm region. A possible reason for this is the low absorptivity of the electronic transitions, supported by TDDFT calculations (see below). This is addressed by first establishing an electronic structure using DFT computations and then calculating the electronic transitions using the TDDFT approach. Selected molecular orbital (MO) representations for $Cl[Ag_2(PhPPy_2)_2Cl]_n$ oligomers (n = 1, 2, 7) are shown in Figures 5 and 6 and were calculated using the X-ray data as input files. The cases with n = 3 and 5 are included with the Supporting Information (Figures S1 and S2).

In all cases, the lowest unoccupied MOs (LUMOs) are π^* orbitals primarily localized on the pyridine rings of the $PhPPy_2$ ligands. For the highest occupied MO (HOMO) in the monomeric species, a mixture of σ^*(Ag−Cl) and σ^*(Ag···Ag) are computed as the major and minor contributions, respectively (Figure 5). In the monomer, the σ^*(Ag···Ag) MO is built upon the $d_{x^2-y^2}-d_{x^2-y^2}$

(50) Jaw, H.-R. C.; Savas, M. M.; Rogers, R. D.; Mason, W. R. *Inorg. Chem.* **1989**, *28*, 1028–1037.
(51) (a) Desiraju, G. R. *Angew. Chem., Int. Ed. Engl.* **1995**, *34*, 2311–2327. (b) Han, J.; Yau, C.-W.; Lam, C.-K.; Mak, T. C.-W. *J. Am. Chem. Soc.* **2008**, *130*, 10315–10326. Wu, J.-S.; Leung, K. C.-F.; Benítez, D.; Han, J.-Y.; Cantrill, S. J.; Fang, L.; Stoddart, J. F. *Angew. Chem., Int. Ed.* **2008**, *47*, 7470–7474.
(52) (a) Chandrasekhar, V.; Baskar, V.; Kingsley, S.; Nagendran, S.; Butcher, R. J. *CrystEngComm* **2001**, *17*, 1–3. (b) Bondi, A. *J. Phys. Chem.* **1964**, *68*, 441–451.

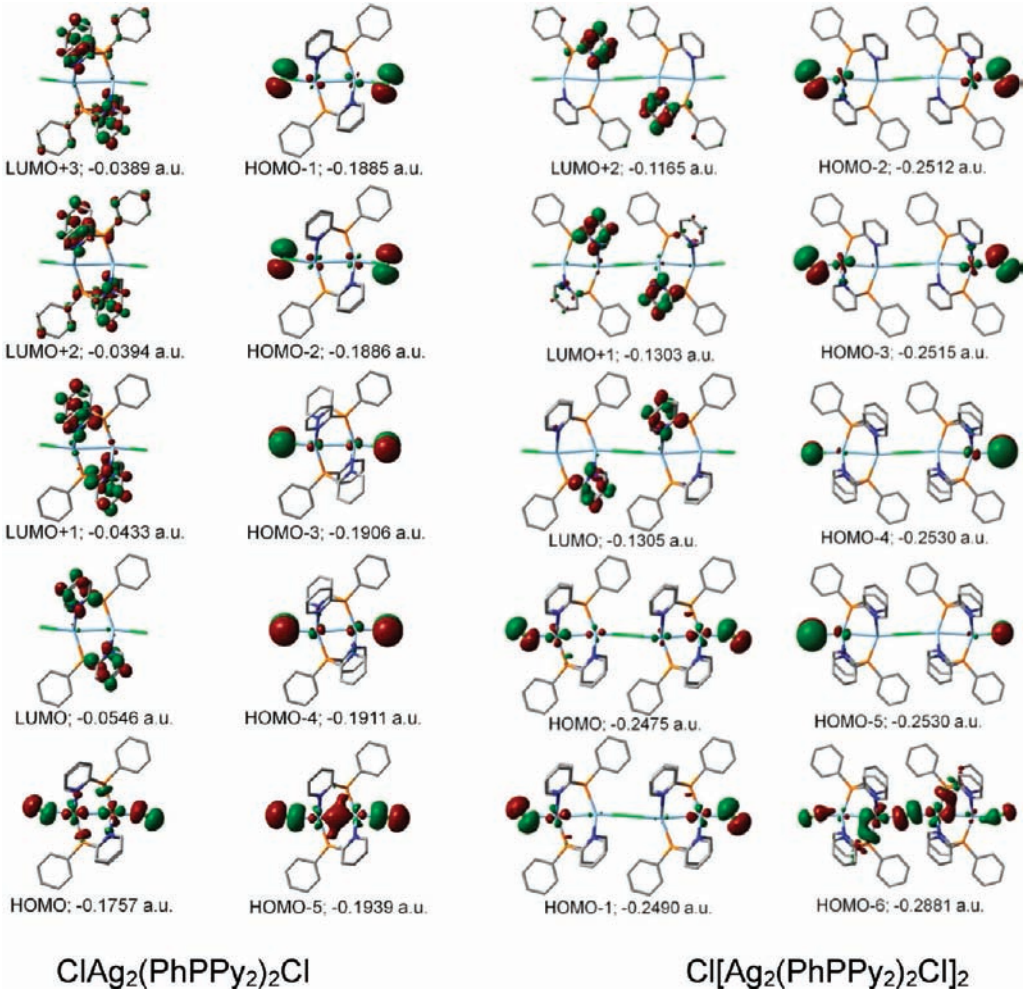

Figure 5. Selected frontier MO representations for the $Cl[Ag_2(PhPPy_2)_2Cl]_n$ units [n = 1 (left), 2 (right)].

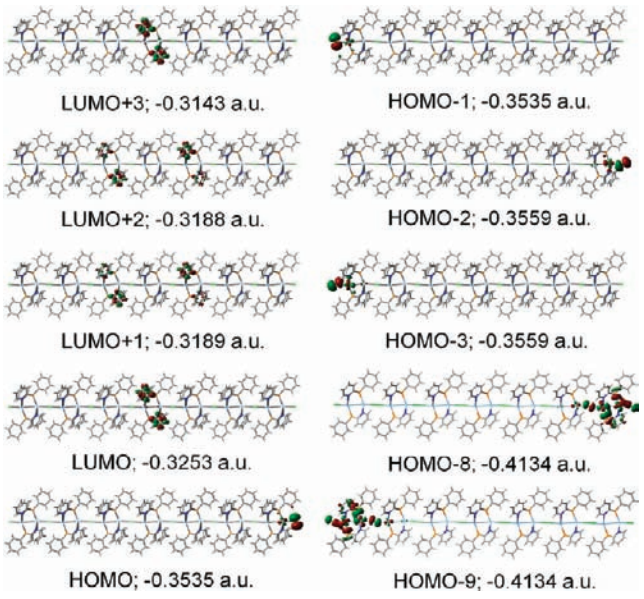

Figure 6. Selected frontier MO representations for the $Cl[Ag_2(PhPPy_2)_2Cl]_n$ units (n = 7).

antibonding interactions, whereas the σ^*(Ag−Cl) MO is constructed with Ag $d_{x^2-y^2}$−Cl p_x interactions (the Ag−Ag vector is placed along the x axis).

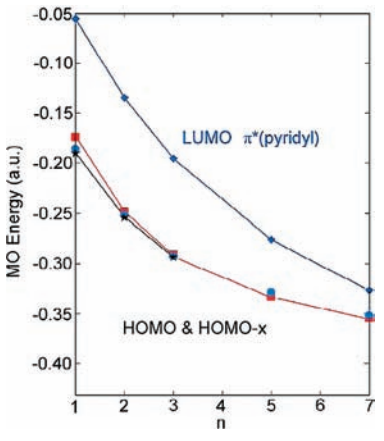

Figure 7. Variation of the MO energy for the frontier orbitals of the $Cl[Ag_2(PhPPy_2)_2Cl]_n$ oligomers (n = 1−3, 5, 7). In HOMO−x, x takes the values of 1−4 for n = 1 and of 1−5 for n = 2, 3, 5, and 7. The square, round, and star dots correspond to the surface MOs issued from antibonding Ag $d_{x^2-y^2}$−Cl p_x, Ag d_{xy}−Cl p_y, and Ag d_{xz}−Cl p_z interactions, respectively.

Below the HOMO, we find two other series of MOs built upon antibonding Ag d_{xy}−Cl p_y (quasi-degenerated HOMO−1 and HOMO−2) and antibonding Ag d_{xz}−Cl p_z interactions (quasi-degenerated HOMO−3 and HOMO−4). HOMO−5 is a mixture of σ^*(Ag−Cl) and

Table 2. Computed Frequency and Wavelength of the 20 First Pure Electronic Transitions for the Monomeric Species $ClAg_2(PhPPy_2)_2Cl$, along with Their Major Individual Contributions

no.	ν (cm^{-1})	λ (nm)	f	major contributions (%)
1	21 504	465.0	0.0427	HOMO → LUMO (99)
2	24 085	415.2	0	HOMO → L+1 (93)
3	24 643	405.8	0.0037	H-1 → LUMO (93)
4	24 667	405.4	0	H-2 → LUMO (93)
5	24 974	400.4	0	H-3 → LUMO (12), HOMO → L+2 (86)
6	25 030	399.5	0.0163	HOMO → L+3 (90)
7	25 125	398.0	0	H-3 → LUMO (81), HOMO → L+2 (13)
8	25 207	396.7	0.0005	H-4 → LUMO (85)
9	25 814	387.4	0	H-5 → LUMO (91)
10	26 797	373.2	0	HOMO → L+4 (97)
11	26 892	371.9	0.0029	HOMO → L+5 (96)
12	27 412	364.8	0	H-1 → L+1 (92)
13	27 466	364.1	0.0034	H-2 → L+1 (92)
14	27 868	358.8	0	H-3 → L+1 (50), H-2 → L+2 (21), H-1 → L+3 (21)
15	27 874	358.8	0	H-4 → L+1 (22), H-2 → L+3 (26), H-1 → L+2 (44)
16	27 967	357.6	0.0001	H-3→L+1 (42), H-2→L+2 (31), H-1→L+3 (23)
17	28 020	356.9	0	H-4 → L+1 (56), H-2 → L+3 (13), H-1 → L+2 (12), HOMO → L+6 (12)
18	28 106	355.8	0	H-5 → L+3 (10), H-4 → L+1 (14), HOMO → L+6 (67)
19	28 343	352.8	0.0017	H-5 → L+2 (17), H-2 → L+2 (14), H-1 → L+3 (14), HOMO → L+7 (52)
20	28 385	352.3	0.0086	H-5 → L+1 (54), H-4 → L+3 (18), H-3 → L+2 (23)

Table 3. Computed Frequency and Wavelength of the 20 First Pure Electronic Transitions for the Dimeric Species $Cl[Ag_2(PhPPy_2)_2Cl]_2$, along with Their Major Individual Contributions

no.	ν (cm^{-1})	λ (nm)	f	major contributions (%)
1	21 162	472.5	0	H-1 → LUMO (36), HOMO → L+1 (56)
2	21 189	471.9	0.0452	H-1 → L+1 (35), HOMO → LUMO (58)
3	22 288	448.7	0.0024	H-3 → L+1 (34), H-2 → LUMO (40)
4	22 289	448.6	0.0005	H-3 → LUMO (35), H-2 → L+1 (39)
5	22 717	440.3	0	H-4 → LUMO (40), H-4 → L+1 (40)
6	22 714	440.3	0	H-5 → LUMO (40), H-5 → L+1 (40)
7	23 652	422.8	0.0002	H-1 → L+1 (52), HOMO → LUMO (40)
8	23 658	422.7	0	H-1 → LUMO (53), HOMO → L+1 (42)
9	24 267	412.1	0.0112	H-1 → L+5 (34), HOMO → L+4 (56)
10	24 293	411.6	0	H-1 → L+4 (41), HOMO → L+5 (51)
11	24 498	408.2	0	H-1 → L+3 (32), HOMO → L+2 (61)
12	24 518	407.9	0.0001	H-3 → L+1 (40), H-2 → LUMO (43)
13	24 519	407.8	0	H-3 → LUMO (42), H-2 → L+1 (41)
14	24 534	407.6	0.0109	H-1 → L+2 (37), HOMO → L+3 (56)
15	24 900	401.6	0.0002	H-3 → L+4 (37), H-2 → L+5 (38)
16	24 902	401.6	0.0016	H-3 → L+5 (34), H-2 → L+4 (41)
17	24 924	401.2	0	H-4 → LUMO (43), H-4 → L+1 (40)
18	24 925	401.2	0	H-5 → LUMO (42), H-5 → L+1 (40)
19	25 341	394.6	0.0011	H-5 → L+5 (16), H-4 → L+4 (44), H-4 → L+5 (25)
20	25 342	394.6	0.0004	H-5 → L+4 (44), H-5 → L+5 (25), H-4 → L+5 (16)

Table 4. Computed Frequency and Wavelength of the 20 First Pure Electronic Transitions for the Trimeric Species $Cl[Ag_2(PhPPy_2)_2Cl]_3$, along with Their Major Individual Contributions

no.	ν (cm^{-1})	λ (nm)	f	major contributions (%)
1	17 239	580.1	0.0003	HOMO → LUMO (94)
2	17 260	579.4	0	H-1 → LUMO (95)
3	17 830	560.9	0.0001	H-2 → LUMO (96)
4	17 840	560.5	0	H-3 → LUMO (96)
5	18 166	550.5	0	H-4 → LUMO (100)
6	18 175	550.2	0	H-5 → LUMO (100)
7	19 691	507.8	0	HOMO → L+1 (94)
8	19 713	507.3	0.0014	H-1 → L+1 (95)
9	20 258	493.6	0.0112	H-2 → L+1 (13), H-2 → L+6 (10), H-1 → L+6 (15), HOMO → L+6 (40)
10	20 273	493.3	0.0196	H-3 → L+1 (17), H-1 → L+6 (12), H-1 → L+7 (29), HOMO → L+7 (21)
11	20 286	493.0	0.0016	H-2 → L+1 (83)
12	20 297	492.7	0.0065	H-3 → L+1 (79)
13	20 615	485.1	0	H-4 → L+1 (99)
14	20 625	484.9	0	H-5 → L+1 (99)
15	20 854	479.5	0	H-1 → L+3 (22), HOMO → L+2 (71)
16	20 862	479.3	0	H-1 → L+2 (62), HOMO → L+3 (32)
17	21 020	475.7	0.0002	H-1 → L+2 (32), HOMO → L+3 (62)
18	21 029	475.5	0	H-1 → L+3 (72), HOMO → L+2 (22)
19	21 055	474.9	0.0009	H-2 → L+6 (61), H-2 → L+7 (13)
20	21 079	474.4	0.0009	H-3 → L+6 (14), H-3 → L+7 (60)

σ(Ag···Ag). For the dimeric species, the HOMO becomes the degenerate HOMO and HOMO−1 (Figure 5) and the lower-energy MOs exhibit the same relative energy order, atomic contribution, and MO character. The same trend is computed for the trimer (Figures S1 in the Supporting Information), but the two sets of HOMO and HOMO−1 and of HOMO−2 and HOMO−3 are closely placed in the energy MO diagram (i.e., nearly accidently degenerated). For the pentamer and heptamer, the reversal of order between these two sets of MOs is then computed and the quasi-degenerated nature of these series remains, as plotted in Figure 7. The energy gap between the LUMO and HOMO decreases with n, suggesting that the lowest-energy electronic transitions should be more shifted to the red as n is increased. Noteworthy, despite the appearance of localized atomic contributions in the MOs (Figures 5, 6, and S1 and S2 in the Supporting Information), hence indicating that the polymer is obviously unconjugated, which is consistent with the closed shell of the Ag and Cl ions, Figure 7 illustrates that the addition of supplementary units in the oligomers has a stabilizing effect.

One other important issue that is noted upon further examination of Figures 5 and 6 is that again the MOs appear to be localized on one unit or another. Second, the atomic contributions on the frontier LUMOs and HOMOs are very different in nature (i.e., very poor orbital overlap). From these two observations, the oscillator strengths for the electronic transitions are predicted to be very weak on the basis of orbital overlaps. This is indeed the case as depicted in Tables 2−4 where about half of the first electronic transitions exhibit calculated oscillator strengths (f) of zero. The others are small. Together, the absence of a transition and the weakness

of the others make the overall predicted spectrum of weak intensity. This observation would explain why the solid is colorless.

Through calculation of enough pure electronic (0,0) transitions (here 100 is the maximum), a graph of the absorptivity or oscillator strengths as a function of the wavelength generates a bar graph (see the green bars in Figure 8). When a thickness assigned to the bar, a calculated spectrum can be generated (see the red trace in Figure 8). The calculated spectrum does not include vibronic components, so they will appear narrow. In reality, they should be broadened by these vibronic features on the high-energy side of the 0−0 component. Nonetheless, the resemblance between the experimental and calculated spectra suggests that the calculations are valid.

The calculated spectrum for one unit, $ClAg_2(PhPPy_2)_2$-Cl, exhibits stronger absorptions below 300 nm and weaker ones above 300 nm. These features lead to a resemblance with the experimental solid-state absorption spectrum (Figure 4). The computed strongest-intensity feature in the low-energy region is found at 465 nm (calculated f = 0.043). For the dimer $Cl[Ag_2(PhPPy_2)_2Cl]_2$, this feature is calculated at 472 nm (f = 0.045). The computed spectrum for the trimer $Cl[Ag_2(PhPPy_2)_2Cl]_3$ exhibits the computed strongest-intensity feature in the low-energy region at 493 nm (f = 0.020). The red shift is consistent with the expected trend based on the reduction of the HOMO−LUMO gap seen in Figure 7. However, an extra new feature (of a much lower intensity; f = 0.0003) is also computed at 580 nm.

The decrease in the calculated oscillator strength on going from 2 to 3 units and the appearance of a weak feature in the 580-nm region are also consistent with the experimental spectrum (Figure 4). Overall, we find that the computed spectra are consistent with the experimental data, and metal/halide-to-pyridyl charge-transfer (M/XLCT) assignments for the lowest-energy absorption bands are made on the basis of the DFT and TDDFT calculations.

Although complexes containing phosphorus and nitrogen ligands are numerous,[53] only a few have been reported to be luminescent.[54,55] The $\{[Ag_2(PhPPy_2)_2Cl](ClO_4)\}_n$ polymer is found to be luminescent in the solid state at room temperature (Figure 9). The most striking feature is that the emission is localized between 400 and 600 nm (with a maximum at ~520 nm), a range where absorption features are still present. The presence of luminescence in this specific range is consistent with what has been reported for other phosphorus- and nitrogen-ligand-containing binuclear silver and copper complexes.[54,55] The presence of shoulders on the high-energy side of the emission suggests that it may be ligand-localized. This was verified using the pure ligand in the solid state (Figure S3 in the Supporting Information), and indeed shoulders are also observed on the high-energy side as well. The overall shape of these emissions for both ligands is consistent with the proposed assignment of the absorption bands (i.e., M/XLCT). The polymer emission is red-shifted with respect to the uncoordinated ligand. This behavior is common, and numerous examples where coordination of a ligand onto a transition metal with a d^{10} electronic configuration exist.[56]

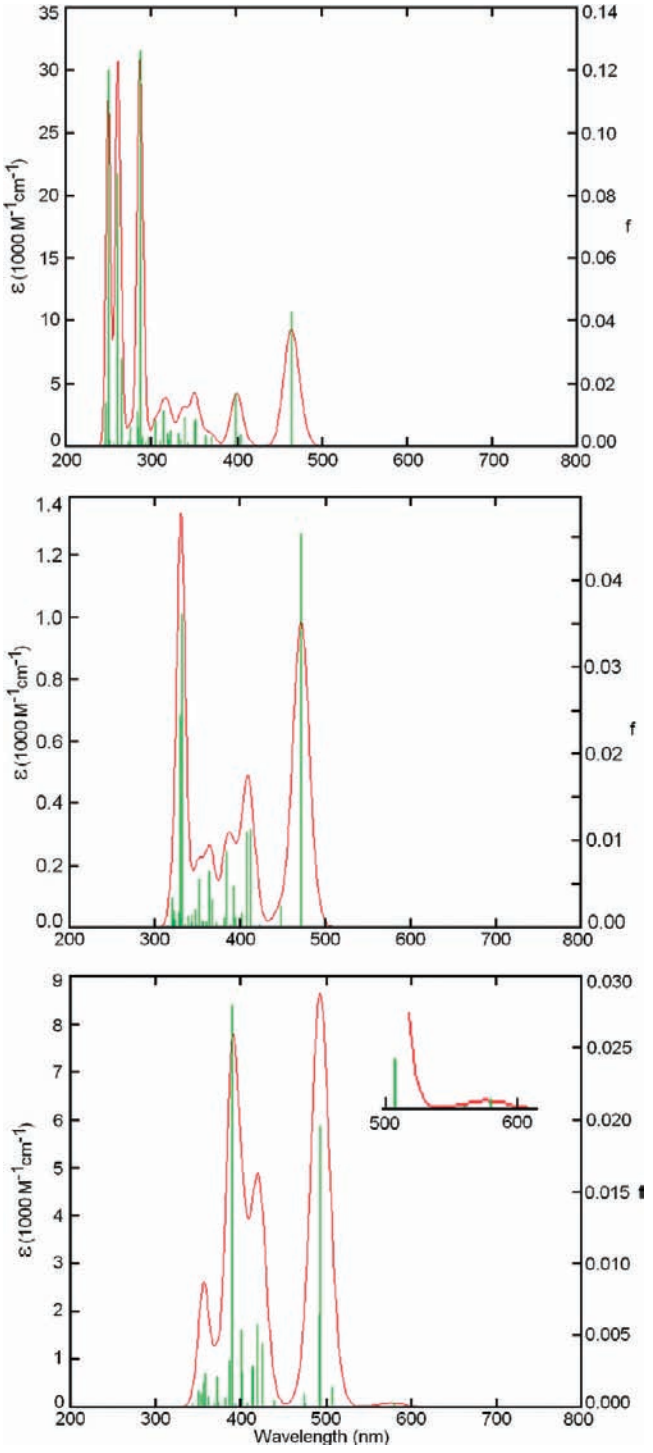

Figure 8. Computed absorption spectra of the monomer and trimer of $Cl[Ag_2(PhPPy_2)_2Cl]_n$ [n = 1 (top), 2 (middle), 3 (bottom)]. Green = bar graph; red = spectrum with an assigned thickness of 1000 cm^{-1}.

(53) Maggini, S. *Coord. Chem. Rev.* **2009**, *253*, 1793–1832.
(54) Catalano, V. J.; Horner, S. J. *Inorg. Chem.* **2003**, *42*, 8430–8438.
(55) Crespo, O.; Gimeno, M. C.; Laguna, A.; Larraz, C. *Z. Naturforsch.* **2009**, *64b*, 1525–1534.
(56) Guyon, F.; Hameau, A.; Khatyr, A.; Knorr, M.; Amrouche, H.; Fortin, D.; Harvey, P. D.; Strohmann, C.; Ndiaye, A. L.; Huch, V.; Veith, M.; Avarvari, N. *Inorg. Chem.* **2008**, *47*, 7483–7492.

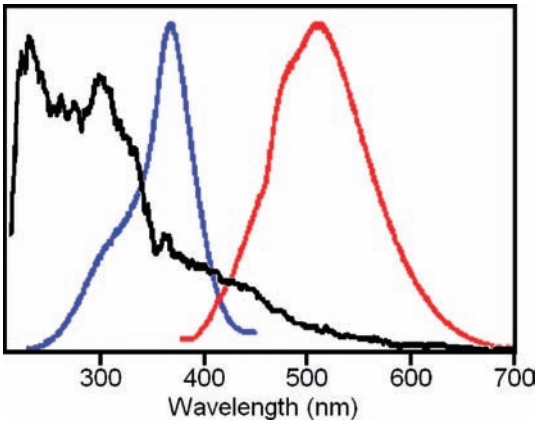

Figure 9. Comparison of the solid-state absorption (black), excitation (blue), and emission spectra (red) of $([Ag_2(PPhPy_2)_2]Cl(ClO_4))_n$ at 298 K.

The emission spectrum curiously begins at 400 nm, which is significantly blue-shifted with respect to the absorption (Figure 9). We considered the possibility that, in the bulk, small oligomers may be present and may be responsible for the observed blue-shifted luminescence. Because of the poor solubility of the bulk material, this could not be verified. No other emission was noted between 700 and 850 nm, which is the limit of the instrument.

Conclusion

An original new 1D coordination polymer of the type $(MMX)_n$ has been synthesized and characterized. Its novelty arises from the use of silver, and its structure exhibits a trigonal-bipyramidal geometry about the metal. Surprisingly, the monomeric bimetallic complex has never been prepared, conversely to its congener $Cu_2(PhPPy_2)_2Cl_2$.[51] The particularly poor solubility of the $\{[Ag_2(PPhPy_2)_2]Cl(ClO_4)\}_n$ polymer may explain this notable difference, a difference that may be associated with the covalent nature of the Ag−Cl bond. The strong Ag−Cl interaction could also be noted in the frontier MO representations. During the course of this study, the presence of luminescence for this colorless polymer prompted us to examine the electronic spectra and their interpretation by means of DFT and TDDFT calculations. M/XLCT assignments were made to explain the presence of weak absorptions in the visible region of the spectrum, electronic transitions that exhibit strong forbidden character. The striking feature is the presence of luminescence centered at 500 nm, which is blue-shifted with respect to the absorption bands. Because the $Ag_2(PhPPy_2)_2Cl_2$ binuclear complex representing a monomer unit could not be isolated, the explanation of this luminescence could not be confidently explained experimentally. This recently synthesized new ligand, $PhPPy_2$, has led us to the preparation of new complexes and now a new and unusual 1D coordination polymer, which exhibits unusual absorption and luminescence properties. Further works are in progress.

Acknowledgment. This research was supported by the National Natural Science Foundation of China (Grant 20871049), the Analytical and Testing Center, Huazhong University of Science and Technology (to T.Z.), the Natural Sciences and Engineering Research Council of Canada, le Fonds Québécois de la Recherche sur la Nature et les Technologies, and the Centre d'Études des Matériaux Optiques et Photoniques de l'Université de Sherbrooke (to P.D.H.).

Supporting Information Available: X-ray crystallographic data file in CIF format, excitation (black) and emission spectra (red) of the $PPhPy_2$ ligand in the solid state at 298 K, and selected frontier MO representations for the $Cl[Ag_2(PhPPy_2)_2Cl]_n$ units ($n = 3, 5$). This material is available free of charge via the Internet at http://pubs.acs.org.